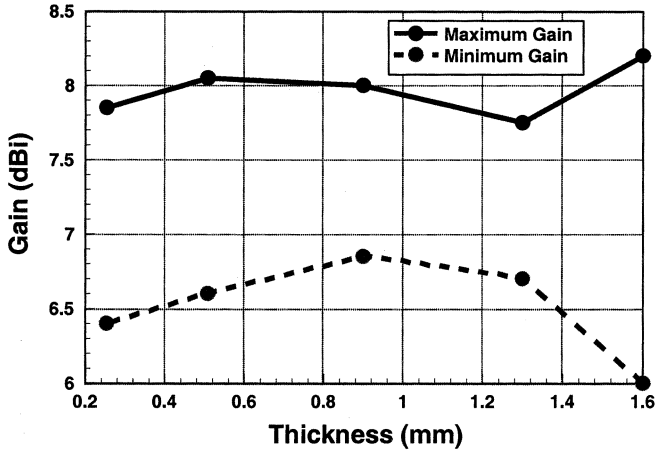

Fig. 7. Maximum and minimum antenna gain versus thickness of feed substrate.

An impedance bandwidth in excess of 27% is obtainable from an ASP antenna that incorporates a thin, high permittivity feed substrate. This bandwidth is not as broad as the ASP antennas in [3] due to the effect of the feed substrate on the resonant coupling aperture. However, the bandwidth is sufficient for a wide range of communications system applications. The gain maintains a level similar to the initial ASP structure that utilizes a low permittivity feed substrate, implying that the surface wave activity remains low.

The impedance bandwidth of the ASP antenna with a high permittivity feed substrate is comparable to that of a frequency scaled version of the OEIC/MMIC compatible hi-lo-lo antenna geometry [7]. The hi-lo-lo structure has the advantage of a ground plane to reduce the level of back radiation, enabling a superior front to back ratio to that of the ASP configuration. However, the ASP ground plane provides isolation between the antenna elements and the feed arrangement, reducing spurious radiation and coupling to other device in the circuit.

As previously stated, the investigation presented here was conducted near 8 GHz. For communication links at lower than this frequency band, in particular low microwave frequencies (less than 4 GHz), direct integration of the printed antenna does not seem feasible. However, in the millimeter-wave band, where several fiber radio/wireless systems are being proposed and developed (for example, [8], [9]) direct integration is a viable, cost effective alternative. For a *Ka* band system, bandwidth values approaching 35% are achievable.

III. Conclusion

The suitability of the microstrip line fed ASP configuration for integration into an OEIC/MMIC module was analyzed in this paper. The effects of altering the properties of the feed substrate on the characteristics of the antenna were investigated. It was found that decreasing the thickness and/or increasing the permittivity of the feed substrate diminished the maximum achievable bandwidth of the antenna. However, ample values of bandwidth (in excess of 27%) and gain were still obtainable using a thickness and permittivity that emulated an OEIC/MMIC wafer.

References

[1] Y. Furuhama, "Research and developments of millimeter-wave technologies for advanced communications," in *Proc. 3rd RIEC Symp. Novel Techniques and Applications of Millimeter-Waves*, Sendai, Japan, Dec. 1998, pp. 1–6.

[2] D. M. Pozar, "Microstrip antennas," *Proc. IEEE*, vol. 80, pp. 79–91, Jan. 1992.

[3] S. D. Targonski, R. B. Waterhouse, and D. M. Pozar, "Design of wide-band aperture-stacked patch microstrip antennas," *IEEE Trans. Antennas Propagat.*, vol. 46, pp. 1245–1251, Sept. 1998.

[4] F. Croq and D. M. Pozar, "Millimeter-wave design of wide-band aperture-coupled stacked microstrip antennas," *IEEE Trans. Antennas Propagat.*, vol. 39, pp. 1770–1776, Dec. 1991.

[5] Ensemble 6.0, in Ansoft, 1999.

[6] R. B. Waterhouse, "Microstrip antennas," in *Handbook on Antennas in Wireless Communications*. Boca Raton, FL: CRC Press, 2001, ch. 6.

[7] W. S. T. Rowe and R. B. Waterhouse, "Broadband microstrip patch antennas for MMICs," *Electron. Lett.*, vol. 36, no. 7, pp. 597–599, 2000.

[8] G. H. Smith *et al.*, "A broadband integrated photonic-antenna interface for multiservice millimeter-wave fiber-wireless applications," in *Proc. IEEE Int. Topical Meeting Microwave Photonics (MWP 2001)*, Long Beach, CA, Jan. 2001, pp. 173–176.

[9] W. D. Jemison *et al.*, "Hybrid fiberoptic-millimeter-wave links," *IEEE Microwave Mag.*, vol. 1, June 2000.

A Relation Between the Active Input Impedance and the Active Element Pattern of a Phased Array

David M. Pozar

***Abstract*—It is well known that the active element pattern of a phased array, obtained by driving a single radiating element of the array while all other elements are match terminated, can be expressed in terms of the scattering matrix parameters of the array. In this paper, it is shown how this relationship can be inverted so that the scattering parameters for all elements of a phased array can be obtained from the active element patterns of the array. In addition, it is also possible to obtain the active input impedance of any element in the fully excited array, at any scan angle, from active element pattern data. The theory is developed for linear and planar arrays and an example is presented for a linear array of slot antenna elements.**

***Index Terms*—Active element pattern, phased arrays.**

I. Introduction

As described in [1]–[3], the active element pattern of a phased array is defined as the radiation pattern of the array when one radiating element is driven and all others are terminated with matched loads. Note that this definition implies that the active element pattern will, in general, depend on the position of the particular fed element in the array. If the array is infinite and uniformly periodic, the active element patterns will be identical for all elements in the array. If the array is finite but large, the active element patterns will be approximately identical for the central elements in the array. The active element pattern has considerable practical importance because the pattern of a fully excited (scanned) phased array can be expressed in terms of the active element patterns and the array factor. If the array is large enough so that the active element patterns can be approximated as identical, pattern multiplication can be used to simply express the fully excited array pattern as the product of the active element pattern and the array factor. Since mutual coupling effects are rigorously included in this procedure, the

Manuscript received August 20, 2002.

The author is with the Electrical and Computer Engineering Department, University of Massachusetts at Amherst, Amherst, MA 01003 USA (e-mail: pozar@ecs.umass.edu).

Digital Object Identifier 10.1109/TAP.2003.816302

0018-926X/03$17.00 © 2003 IEEE

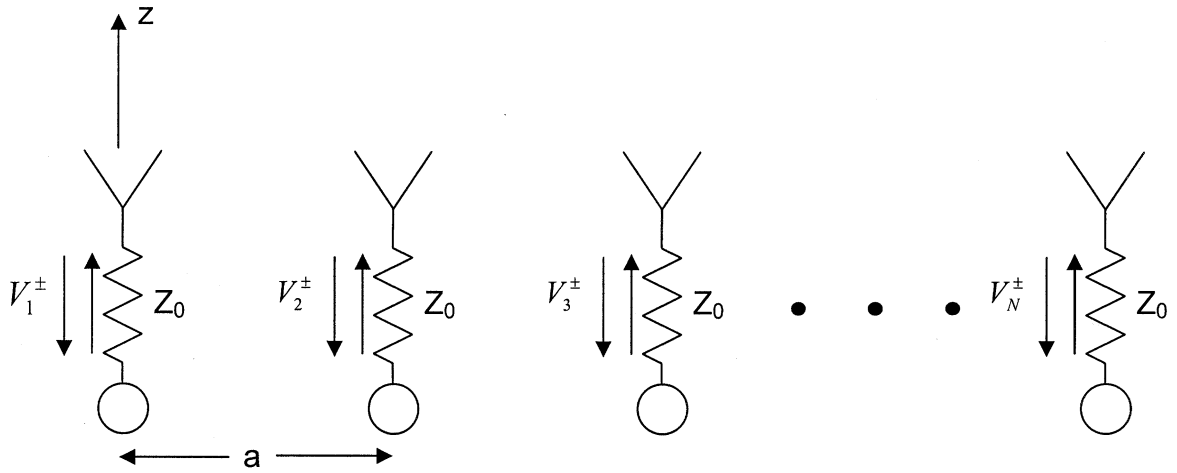

Fig. 1. Geometry of an N element phased array.

actual scan performance (including scan mismatch and blindness effects) of a phased array can be predicted from the active element pattern. It is fairly straightforward to measure active element patterns, even for a large array, since the complication and expense of phase shifters and a feeding network are not required.

It has been shown in [2] and [3] that the active element pattern of an element in a phased array can be mathematically expressed in terms of the scattering parameters of the array and the isolated (nonarrayed) element pattern. In this paper, we show that this representation can be inverted to provide the scattering parameters of the array if the active element patterns are known. In particular, we show that, for an N element array, knowledge of the magnitude and phase of the active element pattern for the mth element at N unique angles will provide the mth column of the $N \times N$ scattering matrix. Additionally, this data can be used to find the active input impedance of the mth element of the fully scanned array at N scan angles. These results apply to both linear and planar arrays. To demonstrate these relationships, data are presented for a five-element array of resonant slot elements.

Recent related work includes the use of measured S parameters to characterize the scanning performance of microstrip patch arrays [4], an experimental method to determine the scan impedance of large arrays [5], and the introduction of specially defined active element patterns that are shown to be related to the mutual impedance matrix of a phased array [6].

II. Derivation of the Relationship Between the Active Element Pattern and the Scattering Matrix of a Phased Array

Initially, we consider an N element linear array fed with voltage generators having internal impedance Z_0, as shown in Fig. 1. The phase reference is taken at the first element and the pattern angle θ is measured from the z axis (normal to the plane of the array).

At the terminals of each element, incident and reflected voltages, V_i^+ and V_i^- are defined. The element feed ports are characterized by the $N \times N$ scattering matrix whose elements are defined as [7]

$$S_{ij} = \left.\frac{V_i^-}{V_j^+}\right|_{V_k^+=0 \text{ for } k\neq j}. \tag{1}$$

The total terminal voltage at the ith element is then

$$V_i = V_i^+ + V_i^- = V_i^+ + \sum_{j=1}^{N} S_{ij} V_i^+. \tag{2}$$

To simplify the derivation, we assume that the radiating elements are *voltage-driven elements*, meaning that the far field produced by a particular element is proportional to the terminal voltage at that element. Then the field radiated by a single element at the origin can be expressed as

$$E_0(r,\theta) = V_0 F(\theta) \frac{e^{-jkr}}{r} \tag{3}$$

where V_0 is the terminal voltage and $F(\theta)$ represents the dominant polarization of the element pattern. Then the total radiated field of the array is given by

$$E^a(r,\theta) = F(\theta)\frac{e^{-jkr}}{r} \sum_{n=1}^{N} V_n e^{j(n-1)u} \tag{4}$$

where $u = ka\ \sin\theta$.

In the fully excited phased-array configuration, scanning to the angle θ_0 requires that the incident voltages at each element be phased as

$$V_n^+ = V_0 e^{-j(n-1)u_0} \tag{5}$$

where $u_0 = ka\ \sin\theta_0$. The resulting field from the scanned array is then given as

$$E^a(r,\theta) = F(\theta)\frac{e^{-jkr}}{r} V_0 \times \sum_{n=1}^{N} \left[e^{-j(n-1)u_0} + \sum_{m=1}^{N} S_{nm} e^{-j(m-1)u_0} \right] e^{j(n-1)u}. \tag{6}$$

The active reflection coefficient seen at element m of the fully excited array is given from (2) and (5) as

$$\Gamma_m(\theta) = \frac{V_m^-}{V_m^+} = \frac{\sum_{n=1}^{N} S_{mn} e^{-j(n-1)u}}{e^{-j(m-1)u}} = \sum_{n=1}^{N} S_{mn} e^{-j(n-m)u}. \tag{7}$$

Now consider the active element pattern of the mth element, for which we set all voltage generators to zero except for the generator at the mth element. Then the incident voltages are given by

$$V_n^+ = \begin{cases} V_0, & \text{for } m = n \\ 0, & \text{for } m \neq n \end{cases} \tag{8}$$

while the reflected voltages are $V_n^- = S_{nm}V_0$. Using (4) and (8) gives the active element pattern of the mth element as

$$E_m^e(r,\theta) = F(\theta)\frac{e^{-jkr}}{r}V_0\left[e^{jk(m-1)u} + \sum_{n=1}^{N} S_{nm}e^{j(n-1)u}\right]. \quad (9)$$

In the usual case where the array elements are passive, $S_{mn} = S_{nm}$ and (7) can be written as

$$\Gamma_m(-\theta) = e^{-j(m-1)u}\sum_{n=1}^{N} S_{nm}e^{j(n-1)u}$$

which allows the active element pattern of (9) to be rewritten as

$$E_m^e(r,\theta) = F(\theta)\frac{e^{-jkr}}{r}V_0\left[1+\Gamma_m(-\theta)\right]e^{j(m-1)u}. \quad (10)$$

Next assume that we are able to measure or calculate the active element pattern at N unique angles θ_i, for $i = 1, 2, 3, \ldots N$. After suppressing the e^{-jkr}/r factor, (10) can be written as a column vector of N elements

$$\begin{bmatrix} E_m^e(\theta_1) \\ \vdots \\ E_m^e(\theta_N) \end{bmatrix} = V_0 \begin{bmatrix} F(\theta_1)\left\{e^{j(m-1)u_1} + \sum_{n=1}^{N} S_{nm}e^{j(n-1)u_1}\right\} \\ \vdots \\ F(\theta_N)\left\{e^{j(m-1)u_N} + \sum_{n=1}^{N} S_{nm}e^{j(n-1)u_N}\right\} \end{bmatrix}$$

where $u_i = ka\sin\theta_i$. In matrix form, this becomes

$$[E_m^e] = V_0[F]\left\{[e_c] + [e_s][S_m]\right\} \quad (11)$$

where $[E_m^e]$ is a column vector of length N, $[F]$ is a diagonal matrix of order N with elements $F(\theta_i)$, $[e_c]$ is a column vector of length N having elements $e_c(i) = e^{j(m-1)u_i}$, $[e_s]$ is a square matrix of order N having elements $e_s(i,n) = e^{j(n-1)u_i}$, and $[S_m]$ is a column vector of length N representing the mth column of the scattering matrix. Equation (11) can be solved for $[S_m]$ as

$$[S_m] = [e_s]^{-1}\left\{\frac{1}{V_0}[F]^{-1}[E_m^e] - [e_c]\right\} = [e_s]^{-1}[A]. \quad (12)$$

The elements of the N element column vector $[A]$ can be simply expressed as

$$A_i = \frac{E_m^e(\theta_i)}{V_0F(\theta_i)} - e^{j(m-1)u_i}. \quad (13)$$

Equation (12) can be applied to each of the N active element patterns of the array, thereby yielding all N columns of the scattering matrix. It is also possible to evaluate the active element pattern at more than N angles and to use a least mean square matrix inversion in (12) to determine the scattering parameters that provide the best fit to the available data in a least mean square error sense.

Using (10), the active reflection coefficient can also be found from active element pattern data and then used to compute the active input impedance at the mth element for the ith scan angle as

$$\begin{aligned} Z_{\text{in}}^m(-\theta_i) &= Z_0\frac{1+\Gamma_m(-\theta_i)}{1-\Gamma_m(-\theta_i)} \\ &= Z_0\frac{E_m^e(\theta_i)e^{-j(m-1)u_i}}{2V_0F(\theta_i) - E_m^e(\theta_i)e^{-j(m-1)u_i}}. \end{aligned} \quad (14)$$

Note that, in general, $\Gamma(\theta) \neq \Gamma(-\theta)$ and $Z_{\text{in}}(\theta) \neq Z_{\text{in}}(-\theta)$, except in the case of an infinite array of symmetric elements or the central element of a finite array having an odd number of symmetric elements.

With proper indexing, the above results can easily be generalized to the case of a planar array. Consider a rectangular grid with M elements (columns) along the x axis with spacing a and N elements (rows) along the y axis with spacing b, so that there are a total of $K = M \times N$ elements. Assume that the elements are counted by rows with a single index $k = 1, 2, 3, \ldots K$. Then $i_k = k \bmod M$ is the x index (column) of element k and $j_k = 1 + \text{int}((k-1)/M)$ is the y index (row) of element k. Let $u = ka\sin\theta\cos\phi$ and $v = kb\sin\theta\sin\phi$. Then the radiated field from the phased array [corresponding to (6)] is

$$\begin{aligned} E^a(r,\theta,\phi) = F(\theta,\phi)\frac{e^{-jkr}}{r}V_0\sum_{n=1}^{K}\Big[&e^{-j[(i_n-1)u_0+(j_n-1)v_0]} \\ &+ \sum_{m=1}^{N} S_{nm}e^{-j[(i_m-1)u_0+(j_m-1)v_0]}\Big]e^{j[(i_n-1)u+(j_n-1)v]} \end{aligned} \quad (15)$$

and the expression for the active reflection coefficient [corresponding to (7)] is

$$\Gamma_m(\theta,\phi) = \sum_{n=1}^{K} S_{mn}e^{-j[(i_n-j_m)u+(j_n-j_m)v]}. \quad (16)$$

The active element pattern of the mth element of the planar array is given by

$$\begin{aligned} E_m^e(r,\theta,\phi) = F(\theta,\phi)\frac{e^{-jkr}}{r}V_0\Big[&e^{j[(i_m-1)u+(j_m-1)v]} \\ &+ \sum_{n=1}^{K} S_{nm}e^{j[(i_n-1)u+(j_n-1)v]}\Big]. \end{aligned} \quad (17)$$

The planar array results that correspond to (12) are formally unchanged, but the matrix elements become $e_c(i) = \exp[j[(i_m-1)u_i + (j_m-1)v_i]]$ and $e_s(i,n) = e[j[(i_n-1)u_i + (j_n-1)v_i]]$ and

$$A_i = \frac{E_m^e(\theta_i,\phi_i)}{V_0F(\theta_i,\phi_i)} - e^{j[(i_m-1)u_i+(j_m-1)v_i]}. \quad (18)$$

Observe that both the active element pattern and the isolated element pattern are required for the above procedures and that these patterns should be measured (or calculated) at the same distance from the antenna and with the same phase reference.

III. Example for a Five–Element Slot Array

As an example to demonstrate the validity of the above results, we consider here a linear array of thin resonant slot elements. Using Booker's relation, the admittance matrix $[Y^s]$ of the slot array can be determined from the moment method impedance matrix $[Z^d]$ of the corresponding wire dipole array [8]

$$[Y^s] = \frac{4}{\eta_0^2}[Z^d] \quad (19)$$

where $\eta_0 = 377\ \Omega$. The impedance matrix of the dipole array can be found using Richmond's piecewise sinusoidal (PWS) moment method solution for thin wire antennas [9]. The admittance matrix of the slot array can be inverted to obtain the port impedance matrix $[Z^s]$ and the scattering matrix obtained as [7]

$$[S] = \left([Z^s] + [Z_0]\right)^{-1}\left([Z^s] - [Z_0]\right) \quad (20)$$

where $[Z_0]$ is a diagonal matrix of the generator impedances. The usual moment method procedure is used to calculate the slot terminal voltages for the case in which a single element is excited (active element pattern) and for the case where all elements are excited with a linear phase progression (phased array). The far field of a $\lambda/2$ slot oriented

TABLE I
CALCULATED ACTIVE ELEMENT PATTERN AND INPUT IMPEDANCE FOR FIVE-SLOT ARRAY

Angle	Active Element Pattern	Active Input Impedance
0°	0.39993< -93.07°	581.51 –j 84.13 Ω
18°	0.41846< 19.53°	667.15 –j 58.26 Ω
36°	0.36533< 113.19	430.22 –j 151.44 Ω
54°	0.28421< 175.74°	181.16 –j 171.00 Ω
72°	0.26195< -142.29°	120.15 –j 166.35 Ω

along the z axis with a PWS current distribution having a peak amplitude of V_0 is given by [8] as

$$E_\phi = \frac{-jV_0}{\pi}\frac{e^{-jkr}}{r}\frac{\cos\left(\frac{\pi}{2}\cos\theta\right)}{\sin\theta} \tag{21}$$

which is used to compute the active element pattern of the mth element of the array. The active input impedance of the phased array case can also be found directly from the moment method procedure.

For a five-element E-plane array of $\lambda/2$ thin slot elements having a spacing of $\lambda/2$, a generator impedance of $Z_0 = 350\ \Omega$ and using one PWS expansion mode per element, the middle column of the scattering matrix is found from (20) as

$$\begin{aligned} S_{13} &= 0.081\,02 < -148.09^\circ \\ S_{23} &= 0.178\,77 < 43.72^\circ \\ S_{33} &= 0.209\,76 < -62.06^\circ \\ S_{43} &= 0.178\,77 < 43.72^\circ \\ S_{53} &= 0.081\,02 < -148.09^\circ. \end{aligned}$$

The active element pattern and the active input impedance for the central element of the array is calculated at five angles using the moment method results as shown in Table I.

With the active element data from Table I, (12) and (14) can be applied to reconstruct the S parameters and active input impedance. Both sets of data are in exact agreement with the previous llisted data.

IV. CONCLUSION

It has been shown how the active element pattern data for a phased array can be used to compute the scattering matrix of the array and the active input impedance of the fully excited array. While these relationships may not be very useful in practice (since S parameters can generally be measured more easily than the magnitude and phase of active element patterns), they help to convey the fundamental importance of the active element pattern and its proper interpretation in terms of mutual coupling and the active input impedance of a phased array.

REFERENCES

[1] P. W. Hannan, "The element-gain paradox for a phased array antenna," *IEEE Trans. Antennas Propagat.*, vol. AP-12, pp. 422–433, July 1964.

[2] D. M. Pozar, "The active element pattern," *IEEE Trans. Antennas Propagat.*, vol. 42, pp. 1176–1178, Aug. 1994.

[3] R. J. Mailloux, *Phased Array Antenna Handbook.* Norwood, MA: Artech House, 1994.

[4] K. Solbach, "Phased array simulation using circular patch radiators," *IEEE Trans. Antennas Propagat.*, vol. 34, pp. 1053–1058, Aug. 1986.

[5] W. Chang, G. J. Wunsch, and D. H. Schaubert, "Back-to-back measurement for characterization of phased-array antennas," *IEEE Trans. Antennas Propagat.*, vol. 48, pp. 1079–1085, July 2000.

[6] D. F. Kelley, "Relationships between active element patterns and mutual impedance matrices in phased array antennas," in *Proc. IEEE Int. Symp. Antennas Propagation Dig.*, June 2002, pp. 524–527.

[7] *Microwave Engineering*, 2nd ed. New York: Wiley , 1997.

[8] R. S. Elliott, *Theory Antenna and Design.* Englewood Cliffs, NJ: Prentice-Hall, 1981.

[9] J. H. Richmond, "Radiation and scattering by thin-wire structures in the complex frequency domain," Ohio State Univ., ElectroScience Lab., Columbus, OH, Tech. Report 2902-10, 1973.

Mutual Coupling Between Patch Antennas Recessed in an Elliptic Cylinder

Chi-Wei Wu, Leo C. Kempel, and Edward J. Rothwell

***Abstract*—The mutual impedance between two rectangular patch antennas recessed in an elliptic cylinder is computed using a finite element-boundary integral method. Results show that the coupling between the antennas is dependent on the curvature of the cylinder surface. For H-plane coupling, the coupling decreases as the radius of curvature increases. For E-plane coupling, the strongest coupling occurs for a specific curvature.**

***Index Terms*—Antenna array mutual coupling, antenna theory, conformal antennas.**

I. INTRODUCTION

Cavity-backed microstrip patch antennas are often used in aircraft applications because of their ability to conform to the vehicle surface. In practical applications, the curvature of the surface must be taken into account in the design of the antennas, since properties such as resonance frequency and impedance are often curvature dependent. For arrays of patches, it is important to be able to predict the dependence on surface curvature of the coupling between patches. In this paper, the mutual impedance between two rectangular cavity-backed patch antennas recessed in an elliptic cylinder is computed using the finite element-boundary integral (FE-BI) method. Since the curvature of an elliptic cylinder varies along one principle direction, the effect of curvature on mutual coupling can be easily studied by placing the antenna array at various positions on the cylinder.

II. THEORY

Consider an infinite, perfectly conducting elliptic cylinder aligned along the z axis. The surface of the cylinder is described by a constant value of the variable u in the elliptic-cylindrical coordinate system. Points on the surface of the cylinder are determined by the angular variable v and the axial variable z. The position $v = 0$ corresponds to the major axis of the ellipse, and, thus, points of greatest surface curvature; $v = \pi/2$ corresponds to the minor axis, and points of least curvature. A perfectly conducting cavity is recessed into the cylinder and filled with a material of permittivity ε such that the aperture of the cavity is flush with the cylinder surface. Two rectangular patches are placed in the aperture, as shown in Fig. 1, and fed with probes carrying uniform current. The probes are placed so that the patches couple along either the E plane or the H plane.

Manuscript received May 29, 2002; revised September 11, 2002.

The authors are with the Department of Electrical and Computer Engineering, Michigan State University East Lansing, MI 48824 USA (e-mail: rothwell@egr.msu.edu).

Digital Object Identifier 10.1109/TAP.2003.816334

0018-926X/03$17.00 © 2003 IEEE